

## EFFECT OF PLASMONIC SILVER NANOPARTICLE ON THE CONVERSION EFFICIENCY OF CHLORIN $e_6$ SENSITISED DYE SOLAR CELLS

ADENIKE, O. OKE; UNO, E. UNO, & MOHAMMED, I. KIMPA

<sup>1</sup>Physics Department, School of Physical Science,  
Federal University of Technology, Minna, Nigeria

E-mail: [bolaoke6@gmail.com](mailto:bolaoke6@gmail.com)

Phone No: +234-703-158-5009

### Abstract

*There is a striking need for an alternative, affordable and renewable energy sources to replace the fossil fuels whose consumption continuously threaten the ecosystem. Consequently, dye-sensitised solar cell (DSSC) is one of the alternative energy sources with immense potential, yet there is still much work to be done before this device can compete with the existing renewable energy technologies. Hence, this work was aimed at fabricating DSSCs using chlorin  $e_6$  as sensitizer. Silver nanoparticles (AgNPs) was incorporated to improve the light harvesting capacity of the device using SILAR method. The optical characteristics of the sensitizer, AgNPs and photoanode of the device were determined using UV-Vis spectrophotometer. Surface morphology of the mesoporous  $TiO_2$  was identified by scanning electron microscope (SEM). Solar simulator under AM 1.5 at 100 mW/cm<sup>2</sup> was used to analyse the conversion efficiency of the device. The optical absorption of chlorin  $e_6$  dye-sensitizer showed absorption peaks at 405, 503, 592 and 664 nm in the visible region. The maximum absorbance wavelengths ( $\lambda_{max}$ ) of AgNPs were observed at 450 and 455 nm for 5 and 10 SILAR cycles respectively; these observed peaks corresponded to peculiar characteristic of the AgNPs surface plasmon resonance band. The optical absorption spectrum of the photo-anode was improved when AgNPs was introduced into the solar cell leading to increase in the absorption intensity. The photovoltaic efficiency of the solar cell with 0, 5 and 10 SILAR cycles of AgNPs were 0.28 %, 0.34 % and 0.43 %. The cell with 10 SILAR cycles of AgNPs exhibiting the highest performing cell in this study.*

**Keywords:** Dye sensitised solar cell, chlorophyll, chlorin  $e_6$ , natural dye,

### Introduction

Global attention in recent years has been shifted towards renewable energy sources including wind, hydro, biomass, geothermal, ocean and solar energies which are perceived to be sustainable as well as promising solution to the emission of greenhouse gases. These gases result from burning of fossil fuel and also will ensure future energy supply that will address current energy crisis (Andersen, 2010; Jolayemi, 2016).

Photovoltaic (PV) technology has been a focal point of research in energy sector, the development of this technology has witnessed different innovative phases, right from the first generation whose technology is based on crystalline silicon (c-Si) and made up of the major current commercial production. On the other hand, the second generation is focused on the thin film technology which covers the range of thin films materials such as cadmium telluride (CdTe), amorphous-silicon (a-Si) and copper (gallium) indium selenide/sulphide (CIGS) (Jolayemi, 2016). The latest innovation involves the multi-junction concepts and emerging fields of optical meta-materials of which Dye-Sensitised Solar Cells (DSSCs) is a key player.

DSSC was first developed by O'Regan and Gratzel (1991), the principle employed organic dyes adsorbed nanocrystalline titanium dioxide ( $TiO_2$ ) films to absorb light from sun and generate electricity. DSSCs technology has been commonly regarded as one of the emerging and most viable candidates for next-generation photovoltaics (Wang and Kitao, 2012). Effort

to enhance the efficiency and improve on the stability of the device is enormously on-going; this includes dye engineering and surface modification of photoanode. Sensitising dye is a crucial parameter in improving the efficiencies of the DSSCs; as a result of its significant role, a growing interest and concerted effort is being channelled towards the development and engineering of efficient and low cost natural dyes to replace the synthetic high-cost dyes with sophisticated preparation techniques (Taya *et al.*, 2013 Mohammed *et al.*, 2015).

On the other hand, surface modification of photoanode is considered as an important way of enhancing the efficiencies of the device and one of the several means of achieving this is the incorporation of plasmonic nanomaterials (Isah *et al.*, 2016). The introduction of these materials into the configuration of the solar cells has been reported to have significantly improved the device efficiencies owing to their localised surface plasmon (LSP) effect (Jolayemi, 2016; Isah *et al.*, 2016; Xu *et al.*, 2013). The localised surface plasma (LSP) effect is one of the most captivating features of these nanomaterials with the ability to strongly absorb and scatter radiation in the visible region (Jolayemi, 2016; Jing *et al.*, 2013).

Chlorophylls function as the key materials for natural photosynthesis which are the most abundant cyclic-tetrapyrrole-based molecules on the Earth (Amao and Komori, 2004). Chlorophyll is an effective photosensitiser in photosynthesis of green plant and an attractive compound as a good photosensitiser in visible region with maximum absorption at 670 nm (Scheer, 1991). As a result of the anchoring unit of this compound, chlorin-based chlorophylls are more suitable for DSSC applications and at the same time they do not contain a heavy metal ion which could pose a problem from environmental point of view (Amao and Komori, 2004). Chlorin  $e_6$  was used as the dye-sensitiser in this study to fabricate dye sensitised solar cell (DSSC).

## **Materials and Methods**

### **Preparation of Photoanode**

The layer of mesoporous  $\text{TiO}_2$ , dye and plasmonic silver nanoparticles on conducting glass substrate (Fluorine doped tin oxide (FTO) glass) forms the photoanode of the device. The preparation of the photoanode started with the cleaning and degreasing of  $2.5 \times 2.5 \text{ cm}^2$  FTO glass with soap (Sodium Lauryl), rinsed with distilled water, ethanol and allowed to dry naturally.

### **Sensitisation of photo-anode**

The prepared layer of AgNPs and  $\text{TiO}_2$  on FTO glass substrates were soaked in the sensitising dye containing chlorin  $e_6$  for about 18 hours for photoanode impregnation, after which the photoanodes were rinsed with ethanol in order to remove excess dye particles that were not properly adsorbed.

The deposition processes for 5 and 10 SILAR cycle is show in Figure 1. Afterwards, a very thin layer of m- $\text{TiO}_2$  was deposited on the plasmonic AgNPs, sintered at  $500^\circ\text{C}$  for 30 min to protect it from the corrosive electrolyte. This process was repeated for another electrode with 5 and 10 SILAR cycles. Then soak the cells in the dye (chlorin  $e_6$ ) for 18 hours, rinse toluene and allow it to dry at  $100^\circ\text{C}$  in an open air for 5 minute.

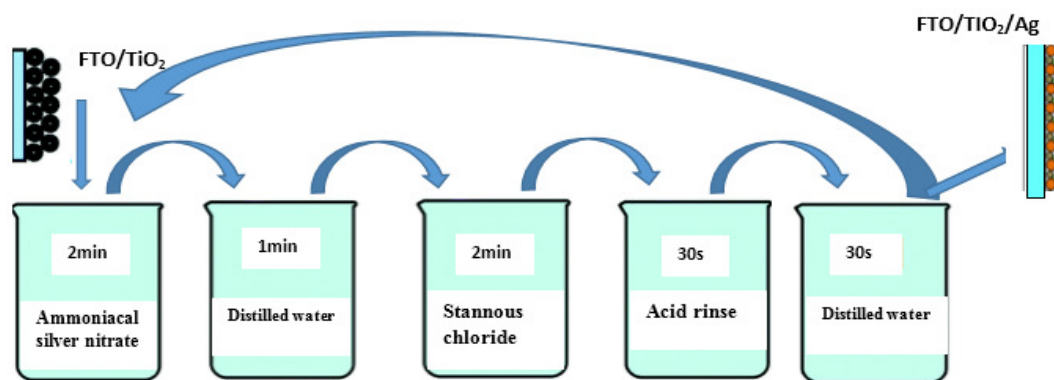


**Figure 1: SILAR cycle process of Silver nanoparticles deposition for DSSC application**

### Assembling of DSSCs

A sandwich-type DSSCs were fabricated by assembling the dye impregnated photoelectrodes and counter-electrodes in an overlapping manner so as to establish electrical connection between the cells and the photovoltaic measurement equipment. The assembling was achieved by using hot-melt sealing gasket of surlyn based polymer sheet (SX1170-25PF, Solaronix) and sealed on a heating stage leaving a pinhole for the electrolyte injection for a few seconds. And finally, the iodine based liquid electrolyte (iodolyte) was injected using micropipette before sealing with hot-melt sealing gasket.

### Material Characterisations

U-Vis spectrophotometer (UV 752 N, Axiom) was used to measure the optical absorption of the dye in the visible region,  $\text{TiO}_2$  photoelectrode and silver nanoparticle composite. The current-voltage characteristics of each cell were recorded with a solar simulator, Keithley 2400-SCS source meter using 300 W xenon light source (Newport Oriel 91160-1000) equipped with AM1.5 filter, which was focused to give a light intensity of  $100 \text{ mW/cm}^2$ , on the surface of dye-sensitised  $\text{TiO}_2$  photoanodes.

### Results and Discussion

#### Optical characterisation of a solar cell

The absorption spectra of the sensitizer dye of Chlorin  $e_6$  in the visible region is shown in Figure 2 with maximum absorption peaks at 405, 503, 592 and 664 nm.

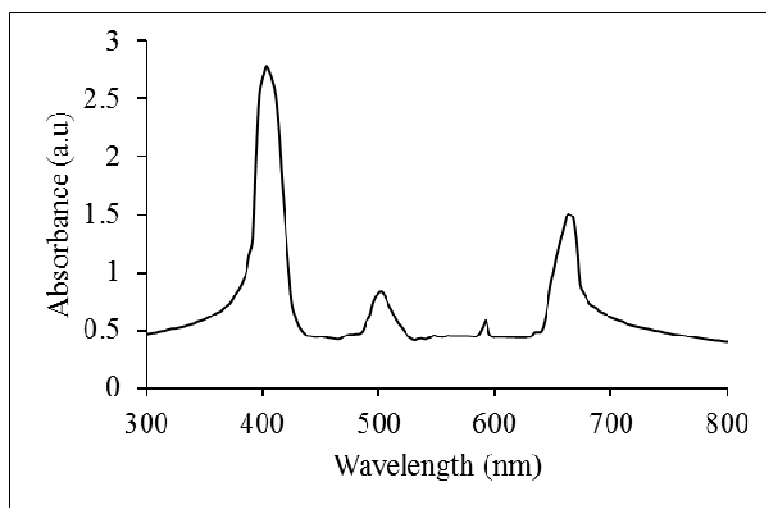


**Figure 2: Absorption spectra of the Chlorin  $e_6$  based dye**

This result indicates that Chlorin  $e_6$  as dye sensitizer has potential to function as semiconductors  $\text{TiO}_2$  with wide band gap using visible light for sensitisation to achieve high photovoltaic efficiency solar cell. A similar work was carried out using chlorin  $e_6$  as dye sensitizer and there was an improvement in overall conversion efficiency (Amao and Komori, 2004; Lightbourne *et al.*, 2015).

The UV-Vis absorption spectra of as-synthesised silver nanoparticles on glass substrate for 5, and 10 SILAR cycles are shown in Figure 3.

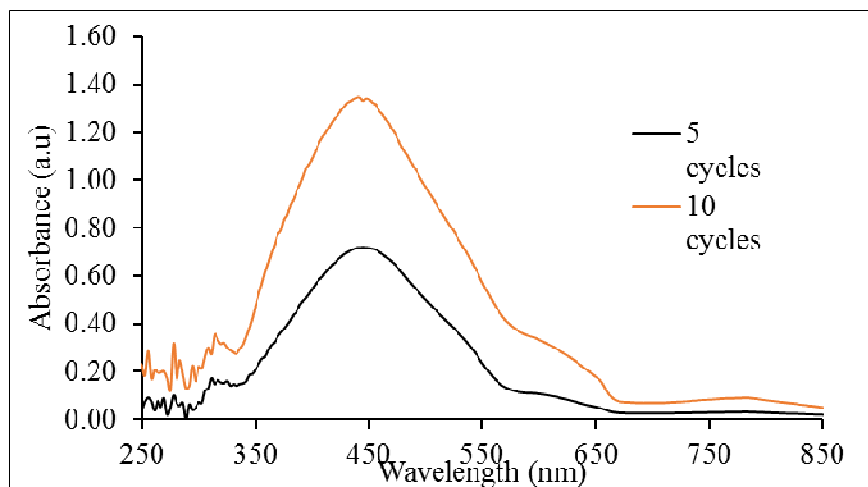


**Figure 3: Optical absorption spectra of AgNPs on glass substrates at different SILAR cycles**

From the absorption spectra that the maximum absorbance wavelengths ( $\lambda_{\text{max}}$ ) are 450 and 455 nm for 5 and 10 SILAR cycles respectively. There is a red shift from 450 to 455 nm by increasing the SILAR cycles from 5 to 10 cycles. This red shift may be attributed to the increasing in size of the nanoparticles by increasing the SILAR cycles as a result of coalescence of Ag nanoparticles at higher SILAR deposition cycles (Gharibshahi *et al.*, 2017; Isah *et al.*, 2016; Zong *et al.*, 2014).

#### **Optical characterisation of photoanode $\text{TiO}_2/\text{AgNPs}$**

The optical spectra of the photoanode containing mesoporous  $\text{TiO}_2$  and plasmonic silver nanoparticles with 5 and 10 SILAR cycles are presented in Figure 4.

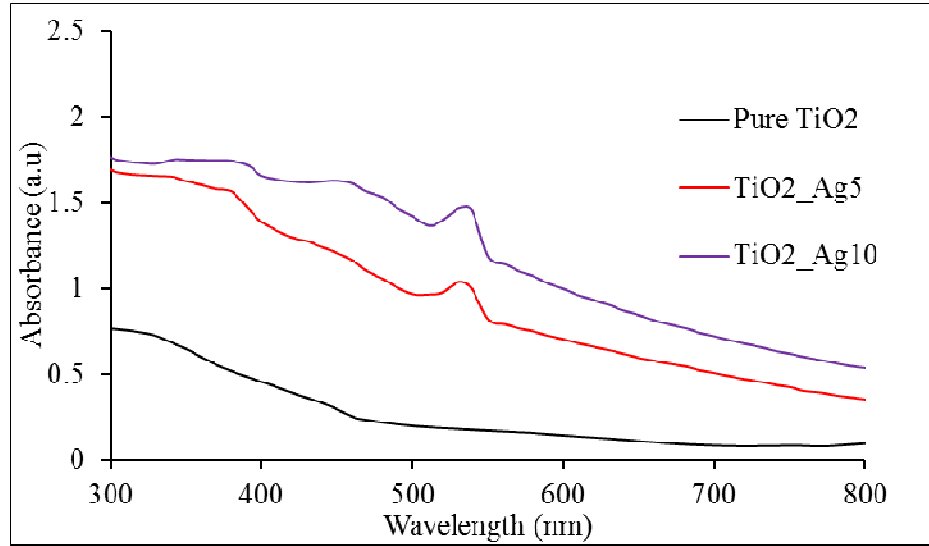


**Figure 4: Absorption spectra of AgNPs SILAR incorporated mesoporous TiO<sub>2</sub>**

The absorption spectrum of the mesoporous TiO<sub>2</sub> (Figure 3) indicates low absorbance at the visible and near infrared regions but shows a strong absorption at the UV region with a broad peak around 300 nm. Figure 4 shows the absorption spectra of the photoanode (m-TiO<sub>2</sub>) containing AgNPs with 5 and 10 SILAR cycles; with the presence of the AgNPs, the spectra indicate improvement in the light absorption capability of the photoanode across the entire UV-Visible spectrum leading to increase in the absorption intensity. The intensity increases as the SILAR cycles increase from 5 to 10. The photoanodes exhibit sharp absorption peak at 530 nm in the visible region. The absorption improvement can be attributed to localized surface plasmons (LSP) effect of the AgNPs (Isah *et al.*, 2016).

#### Current-Voltage (J-V) Characteristics analysis

The current-voltage (J-V) measurement of the solar cells evaluates the effective performance efficiency of the cell. The J-V curve characteristics of the DSSCs exploring Chlorin e<sub>6</sub> dye extract as a sensitizer were determined to study the effect of plasmonic AgNPs on the photovoltaic performance of the dye-sensitized solar cells. The photovoltaic performance evaluations were achieved through the analysis of open-circuit voltage ( $V_{oc}$ ), short-circuit current ( $J_{sc}$ ), fill factor (FF), and energy conversion efficiency ( $\eta$ ) from the graph shown in Figure 5. The efficiency of the cell was calculated using the following relation in equation (1) and (2).

$$\text{Efficiency}(\eta) = \frac{FF \times V_{oc} J_{sc}}{P_{in}} \times 100\% \quad (1)$$

$$\text{Fill factor}(FF) = \frac{V_{max} \times J_{max}}{V_{oc} J_{sc}} = \frac{P_{max}}{V_{oc} J_{sc}} \quad (2)$$

where  $P_{in} = 100 \text{ mW/cm}^2$ ,  $V_{max}$  and  $J_{max}$  are the voltage and the current density at the maximum power output respectively and  $P_{max}$  is the maximum power output.

Figures 5 (a-c) shows current -Voltage (J-V) and Power-Voltage (P-V) characteristic curves for the incorporated plasmonic AgNPs solar cells at different SILAR cycles. Table 1 show the values of the photovoltaic parameters of the solar cells obtained from the curve through equation (1). The effects of the AgNPs on the performance of the DSSCs illustrated in Figures 3 and 4 indicate significant modifications to the photovoltaic parameters ( $J_{sc}$ ,  $V_{oc}$ , and FF) of the cells as the SILAR cycles were varied and in return, made changes to the

performance efficiency of the cell. DSSC\_Ag0 exhibits 0.28 % efficiency with ( $J_{sc} = 1.07$  mA,  $V_{oc} = 0.46$  V, and  $FF = 0.57$ ) which is taken as the reference cell and Ag NPs was incorporated into the cell configuration with 5 SILAR cycles the efficiency increased to 0.34 % with ( $J_{sc} = 1.20$  mA,  $V_{oc} = 0.49$  V, and  $FF = 0.58$ ), increasing the cycles to 10 as well increased the efficiency further to 0.43 % ( $J_{sc} = 1.39$  mA,  $V_{oc} = 0.50$  V, and  $FF = 0.62$ ). Considering these effect, the efficiency experiences different level of enhancements with the different cycles, about 21 % improvement was achieved when 5 SILAR cycles of AgNPs was introduced over the reference cell, DSSC\_Ag0. DSSC\_Ag10 with photovoltaic efficiency of 0.43 % exhibits the highest improvement and came out best performing cells amongst the cells considered with about 54 % improvement over DSSC\_Ag0. As can be observed from table 1, as the SILAR cycle of AgNPs increases from 0 to 10 cycle, the conversion efficiency of the solar cell also increased from 0.28 % to 0.43 % with 10 SILAR cycle having the highest photovoltaic efficiency. Figure 6 shows the J-V characteristics curve in order to explicitly explain and compare their efficiency at various SILAR cycle.

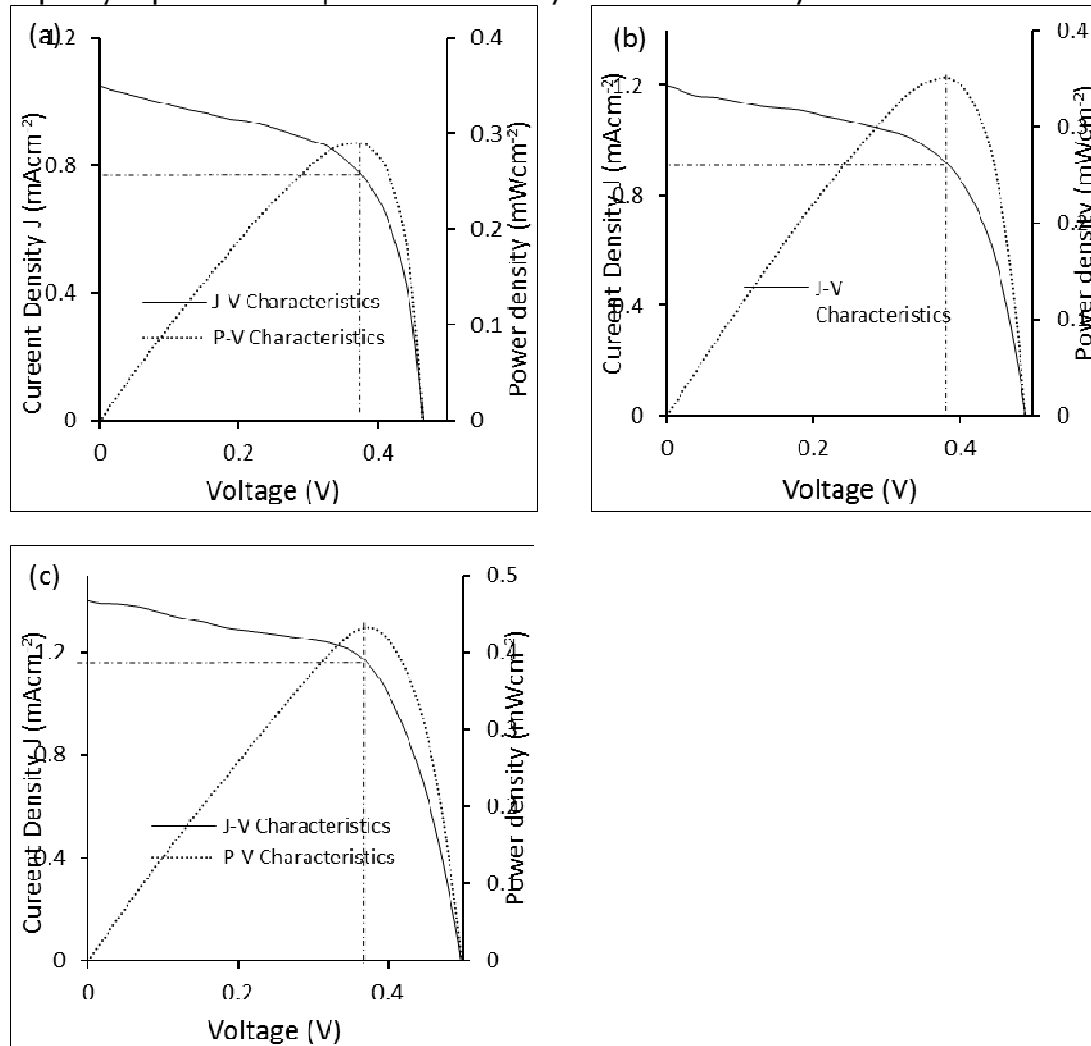


**Figure 5: J-V and P-V characteristics of (a) AgNPs-free DSSC (b) DSSC\_Ag5 (c) DSSC\_Ag10**

**Table 1: Photovoltaic parameters of DSSCs with different Ag SILAR cycles**

S/No	SILAR Cycles	$J_{sc}$ (mA)	$V_{oc}$ (V)	FF	$\eta$ (%)	% increase in $\eta$
1	0	1.07	0.46	0.57	0.28	0.00
2	5	1.20	0.49	0.58	0.34	21.43
3	10	1.39	0.50	0.62	0.43	53.57

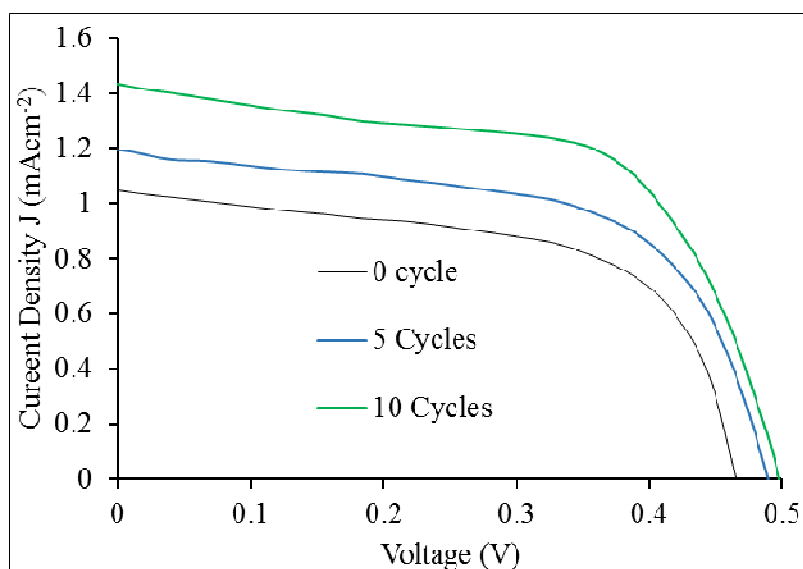


Figure 6: Comparison of the cells performance efficiencies at different SILAR cycles

### Conclusion

In this study, DSSCs have been fabricated using chlorin  $e_6$  as dye sensitizer to improve the light harvesting capacity of solar cell by incorporating AgNPs into the configuration. SILAR method was used to incorporate the AgNPs into the fabricated dye sensitized solar cells using chlorin  $e_6$  as sensitizer. The introduction of AgNPs indicated significant modifications to the photovoltaic parameters ( $J_{sc}$ ,  $V_{oc}$ , and FF) and performance efficiency with respect to the SILAR cycles. DSSC without AgNPs exhibited 0.28 % efficiency ( $J_{sc} = 1.07$  mA,  $V_{oc} = 0.46$  V, and FF= 0.57), increasing the cycles to 10 as well increased the efficiency further to 0.43 % ( $J_{sc} = 1.39$  mA,  $V_{oc} = 0.50$  V, and FF= 0.62).

### References

- Amao, Y., & Komori, T. (2004). Bio-photovoltaic conversion device using chlorine- $e_6$  derived from chlorophyll from *Spirulina* adsorbed on nanocrystalline  $TiO_2$  film electrode. *Biosensors and Bioelectronics*, 19, 843–847.
- Andersen, T. R. (2010). *Organic solar cells—design, synthesis and characterization of novel electron acceptor*. Aalborg, Denmark: Department of biotechnology, chemistry and environmental engineering, Aalborg University.
- Gharibshahi, L., Saion, E., Gharibshahi, E., Shaari, A. H., & Matori, K. A. (2017). Structural and optical properties of Ag nanoparticles synthesized by thermal treatment method. *Materials*, 10(402), 1 – 13.
- Isah, K. U., Jolayemi, B. J., Ahmadu, U., Kimpa, M. I., & Alu, N. (2016). Plasmonic effect of silver nanoparticles intercalated into mesoporous betalain-sensitized- $TiO_2$  film

- electrodes on photovoltaic performance of dye-sensitized solar cells. *Materials for Renewable and Sustainable Energy*, 5 (10), 1-10.
- Jing, H., Zhang, L., & Wang, H. (2013). Geometrically tunable optical properties of metal nanoparticles. In C. S. Kumar, *UV-VIS and photoluminescence spectroscopy for nanomaterials Characterization* (pp. 1-74). Berlin: Springer.
- Jolayemi, J. B. (2016). *Facile synthesis of plasmonic silver nanoparticles and application in dye sensitised solar cells*. Minna: Department of Physics, Federal University of Technology, Minna.
- Lightbourne, S. K., Gobeze, H. B., Subbaiyan, N. K., & D'Souza, F. (2015). Chlorin e6 sensitized photovoltaic cells: Effect of co-adsorbents on cell performance, charge transfer resistance, and charge recombination dynamics. *Journal of Photonics for Energy*, 5, 053089-1 - 053089-11.
- Mohammed, I. K., Kasim, U. I., Yabagi, J. A., & Taufiq, S. (2015). The effect of extracting solvents using natural dye extracts from *hyphaene thabaica* for dye-sensitized solar cells. *Journal of Material Science and Engineering* 4:208, 4-6
- O'Regan, B., & Gratzel, M. (1991). A low-cost, high-efficiency solar cell based on dye sensitized colloidal TiO<sub>2</sub> films. *Nature*, 353, 737–740.
- Scheer, H. (1991). *Chlorophylls*. London: CRC Press.
- Taya, S. A., El-Agez, T. M., El-Ghamri, H. S., & Abdel-Latif, M. (2013). Dye-sensitized solar cells using fresh and dried natural dyes. *International Journal of Materials Science and Applications*, 2 (2), 37-42.
- Wang, X. F., & Kitao, O. (2012). Natural Chlorophyll-Related Porphyrins and Chlorins for Dye-Sensitized Solar Cells. *Molecules*, 17, 4484-4497.
- Xu, Q., Liu, F., Liu, Y., Cui, K., Feng, X. Z., & Huang, Y. (2013). Broadband light absorption enhancement in dye-sensitized solar cells with Au–Ag alloy popcorn nanoparticles. *Scientific Reports*, 3, 1-7.
- Zong, R., Wang, X., Shi, S., & Zhu, Y. (2014). Kinetically controlled seed-mediated growth of narrow dispersed silver nanoparticles up to 120 nm: secondary nucleation, size focusing, and Ostwald ripening. *Physical chemistry chemical physics*, 16, 4236 - 4241.